The Journal of Neuroscience, August 15, 1999, *19*(16):7089–7099

Maps of Central Visual Space in Ferret V1 and V2 Lack Matching Inputs from the Two Eyes

Leonard E. White, William H. Bosking, S. Mark Williams, and David Fitzpatrick

Department of Neurobiology, Duke University Medical Center, Durham, North Carolina 27710

In the visual cortex, the representation of central visual space is supplied by matching geniculate inputs that are driven exclusively by one eye or the other. In layer 4 of early visual areas (V1 in primates and V1 and V2 in cat), these inputs form a nearly uniform array of small ocular dominance domains, while preserving overall topographic order within the cortical map. In ferret, however, ocular dominance domains in different regions of the visual cortex are strikingly irregular in size and shape. The exceptionally large size of domains in some regions implies a departure from the usual visuotopic matching of inputs from the two eyes. Using optical-imaging, electrophysiological, and anatomical techniques, we show that this regional variation is attributable to exclusively monocular maps of the central portions of the ipsilateral visual field in V1 and the contralateral visual field in V2. In addition, we document a complex interdigitation of V1 and V2 that entails a discontinuity in the mapping of visual space and fragmentation of V2 into isolated cortical territories. We suggest that both the monocularity of these cortical maps and the visuotopic discontinuity along the V1–V2 border derive from asymmetries in the crossed and uncrossed retinal pathways.

Key words: striate cortex; optical imaging; V1; V2; lateral geniculate nucleus; ferret

The portion of neocortex in mammals that is devoted to processing visual information comprises a number of separate areas, each of which contains an orderly representation of visual space. In early visual areas (V1 of primates and V1 and V2 of carnivores), these visuotopic maps are established by the systematic distribution of arbors from the lateral geniculate nucleus (LGN) within cortical layer 4. For the representation of central regions of visual space, an additional constraint is imposed on the termination of LGN arbors: the need to map inputs from two sets of LGN neurons that represent the same area of visual space but are driven by different eyes. For most carnivores and primates examined, the result is an approximately uniform pattern of alternating left eye and right eye patches in layer 4, called ocular dominance columns or domains. Although the functional significance of these domains remains uncertain, their small size and uniform distribution establish the framework for local cortical interactions. This arrangement ensures that a given location in cortex will have access to nearby sites that represent adjacent areas of visual space that are driven by the same eye, as well as sites that represent the same region of space but are driven by the other eye. As a result, the distribution of geniculate afferents enables a rich set of monocular and binocular computations for each point in visual space, with minimal disruption of visuotopic continuity across the cortical map (Hubel and Wiesel, 1977; Durbin and Mitchison, 1990; Swindale, 1996; Erwin and Miller, 1998).

The organization of ocular dominance domains in the visual cortex of the ferret, however, exhibits an unusual degree of regional variation in size and shape, unlike that reported in primates (Horton and Hocking, 1996) and cats (Anderson et al., 1988). In the caudal pole of the hemisphere, domains tend to be small and patchy (Law et al., 1988; Redies et al., 1990), comparable to the configuration in cat. In contrast, domains in more rostral portions of occipital cortex are considerably larger (>1 mm in width), are more irregular in shape, and may extend for several millimeters or more in the medial-to-lateral axis of the hemisphere (White et al., 1997). This regional variation in ocular dominance structure raises questions about how visual space is mapped across the visual cortex and whether the same monocular and binocular computations are possible in each region. The goal of this study was to address these questions and shed light on the factor(s) that might account for this arrangement of ocular dominance domains. To do so, we used a combination of physiological and anatomical techniques to examine the relation between the layout of ocular dominance domains and maps of visual space. Our results demonstrate that the large size of the domains reflects the fact that part of the central visual field representation in V1 and the entire representation in V2 are exclusively monocular. Furthermore, significant discontinuities in the mapping of visual space are found along the V1–V2 border, which corresponds to the boundary between these monocular representations.

MATERIALS AND METHODS

All experimental procedures were approved by the Duke University Institutional Animal Care and Use Committee and performed in compliance with guidelines published by the National Institutes of Health. Juvenile and adult European sable ferrets (*Mustela putorius furo*; all older than 40 d; $n > 70$) of both sexes were obtained from Marshall Farms (North Rose, NY). These animals were taken from a "research only" stock of normally pigmented ferrets maintained by the supplier by crossing sable animals; albino ferrets were never breed into this stock.

Ocular dominance domains revealed by transneuronal transport. Ten ferrets were anesthetized with a mixture of ketamine and xylazine, and ~15 μl of 5% (w/v) wheat germ agglutinin–conjugated horseradish peroxidase (WGA-HRP) dissolved in normal saline was slowly infused into the posterior chamber of one eye. After 2–4 d, the ferrets were deeply anesthetized and perfused transcardially with 0.1 M PBS, 4.0%

Received March 17, 1999; revised May 27, 1999; accepted June 3, 1999.

This work was supported by EY06729, EY11488, NS29187, and The McKnight Foundation. We thank David Coppola, Justin Crowley, Michele Pucak, and Dale Purves for critical comments and Oren Yishai for the method of optic disk projection.

Correspondence should be addressed to Dr. Leonard E. White, Department of Neurobiology, Duke University Medical Center, Durham, NC 27710.

paraformaldehyde in 0.1 M phosphate buffer, and 10% sucrose in 0.1 M phosphate buffer. Brains were removed and placed in 20% sucrose in 0.1 M phosphate buffer. The following day, the occipital lobe was excised, unfolded, and frozen flat between two Teflon-coated slides separated by 2–3 mm in 2-methylbutane cooled to −40°C. The flattened occipital lobe was then sectioned on a sliding microtome at 50 μm, and the sections were reacted for the demonstration of peroxidase activity (Mesulam, 1978). The sections were mounted onto subbed slides, dehydrated, cleared, coverslipped, and optically scanned using a Polaroid SprintScan 35 (Polaroid, Cambridge, MA). Adobe Photoshop 3.0 or 4.0 (Adobe Systems, Mountain View, CA) was then used to adjust the contrast of the digital images, and a montage was constructed to represent the distribution of ocular dominance domains across the entire visual cortex.

Animal surgery for optical imaging. Ferrets ($n > 50$) were anesthetized, intubated, and secured in a modified stereotaxic frame that left the animal's central field of view unobstructed. During surgery, anesthesia was maintained with 2–3% isoflurane in a 2:1 mixture of nitrous oxide and oxygen, expired carbon dioxide levels were kept near 4.0%, and body temperature was maintained at 37.5°C. A posterior craniotomy was performed, the dura was reflected, and a stainless steel chamber with a glass window was cemented to the skull and filled with normal saline. Paralysis was induced and maintained by systemic infusion of vecuronium bromide (0.3 $mg \cdot kg^{-1} \cdot hr^{-1}$). Each iris was dilated with ophthalmic atropine, and noncorrective contact lenses were placed on the corneas to prevent drying. Ophthalmoscopic evaluation indicated that proper correction of refraction at the viewing distance of 29 cm would require less than ±1 diopter adjustment. Because of this and the fact that optical signals to the mapping stimuli did not vary with more than an order of magnitude change in spatial frequency, poor accommodation was not a limitation in our studies.

Assessment of eye alignment. The optic axis of each eye was determined by first sighting the optic disk with an ophthalmoscope through a hollow tube and then fixing the position of the tube and placing a small laser light source in the center of the tube. The projection of laser light on the stimulus monitor defined the optic axis of the eye. In eight animals, we compared the position of the monocular multiunit receptive fields (see below) for binocular neurons in V1 that gave nearly equal responses to stimulation of each eye. In general, misalignments in the position of the monocular receptive fields were small relative to the size of the receptive fields. The mean offset of receptive field centers ± SD was 2.0 ± 1.1° of azimuth for 12 sites, whereas the long axis of individual receptive fields ranged from 3 to 20°. In each of the eight animals tested, at least one site (10 of the 12 total) showed an offset of monocular receptive fields consistent with slight divergence of the optic axes. Because these offsets were small and our sample in any given case was limited to three sites or less, we did not correct our determination of the vertical meridian to account for this minor divergence. The vertical meridian was simply defined for each ferret as the midpoint between the projections of the two optic disks.

Optical-imaging procedures. Optical imaging of intrinsic signals was accomplished using an enhanced video acquisition system (Optical Imaging, Germantown, NY) consisting of a tandem lens macroscope attached to a low-noise video camera. This technique is based on the fact that changes in the electrical and metabolic activities of cortical cells alter the local optical properties of the cerebral tissue (for review, see Bonhoeffer and Grinvald, 1996). The cortical surface was illuminated with red light (~700 nm), and the recorded signal passed through an analog video enhancement amplifier and was digitized and stored for further processing by software provided by the manufacturer. A separate stimulus computer (386 personal computer with an SGT+ graphics board and STIM software provided by Kaare Christian) was used to present stimuli on a monitor (screen size = 80 × 60°; 8 pixels/°), which was centered within 5° of the midpoint between the projections of the optic axes.

For demonstration of ocular dominance domains, high-contrast rectangular wave gratings (8.75° dark phase/1.25° light phase; 0.1 cycle/°), oriented at an angle of 0, 45, 90, or 135° and panned back and forth (22.5°/sec or 2.8 cycles/sec) along the axis orthogonal to the orientation of the grating, were presented monocularly by covering one eye with a handheld occluder. A single trial consisted of eight conditions: each of the four gratings presented to each eye for 9 sec with the order of the gratings and the viewing eye specified in a pseudorandom sequence. Each stimulus was presented for 9 sec, with data acquired during the final 8 sec to allow for the time lag in intrinsic signal. A total of 10 trials was performed in each animal, and the summed images obtained while the ferret viewed the four gratings with the left eye were subtracted from the summed images obtained while viewing with the right eye. The resulting ocular dominance image consisted of dark and light regions where dark areas responded best to stimulation of the contralateral eye and light areas responded best to stimulation of the ipsilateral eye.

For demonstrating the map of visual space by optical imaging, the stimulus was a counterphasing checkerboard pattern 5° in width and extending across the full height of the monitor. The individual checks were 2.5° on a side and counterphased between black and white at a rate of 1 cycle/sec; the surrounding field was a uniform gray. Each trial consisted of two stimuli, which the animal viewed binocularly: the checkerboard pattern centered at a specified azimuth and the gray surround field alone (as a stimulus blank). As before, data were acquired during the final 8 sec of a 9 sec trial. A total of 10 trials was performed at each of nine positions from 25° to one side of the center of the monitor (contralateral visual field) to 15° to the other side (ipsilateral visual field) in steps of 5° increments. Images acquired while the animal viewed the blank screen were subtracted from those obtained during presentation of the checkerboard pattern. The cortical map of visual space could then be appreciated most effectively by animating the set of difference images in sequence from the peripheral contralateral field to the peripheral ipsilateral field. This was done on a Macintosh computer using the public domain NIH Image program (developed at the National Institutes of Health and available on the Internet at http:/rsb.info.nih.gov/nih-image/). To produce a static view of the visuotopic data set, we calculated a "position preference map" from the set of individual images; this map displays in color code the stimulus position that evoked the maximal response (largest gray level value) for each pixel in the imaging field.

Electrophysiology. In a subset of cases ($n = 15$), a tungsten microelectrode ($r = 8$–14 MΩ) was inserted orthogonal to the pial surface into selected sites chosen with reference to the ocular dominance map. Multiunit activity was recorded at depths of 200–500 μm (cortical layer 3) using a differential amplifier and was displayed on an oscilloscope and audio monitor, and the signals were sent to a personal computer via a Cambridge Electronic Design (CED) 1401*plus* Intelligent Laboratory Interface (CED, Cambridge, UK). The waveforms of individual cortical neurons were discriminated and tabulated using Spike2 software (CED). For each recording site, the optimum orientation and ocular preference of the multiunit activity, including the indiscriminate "hash" displayed on the audio monitor, were determined. Next, the receptive field of the multiunit activity was plotted using a thin light bar on a dark background at the optimum orientation, with the aid of an interactive computer-based protocol developed in STIM software. This was done by moving the bar of light from the periphery toward the center of the receptive field and back again until a minimum discharge was evoked, which was taken to define one side of a rectangular receptive field; the same procedure was then repeated for the remaining three sides. In some experiments, the stimulus was then centered on the plotted receptive field, and the ocular preference of the multiunit activity was assessed quantitatively. This was done by covering one eye and sweeping the bar back and forth over the receptive field eight times; after reversing the eye patch, the procedure was repeated for the other eye. The mean multiunit spike count per trial was then determined, and an ocular dominance index was calculated: (contralateral eye response − ipsilateral eye response)/(contralateral eye response + ipsilateral eye response). Thus, indices approaching +1 indicated complete contralateral eye dominance, values near 0 indicated no ocular bias, and indices approaching −1 indicated complete ipsilateral eye dominance. Typically, sites that were judged subjectively to be monocular gave ocular dominance indices less than −0.85 (ipsilateral eye only) or greater than +0.85 (contralateral eye only). At some of these monocular sites, irregular patterns of spontaneous activity prevented the computed index from reaching −1 or +1.

Demonstration of geniculocortical inputs. In some experiments ($n = 10$), retrograde axonal tracers were placed in selected cortical targets to establish the source of geniculate input to sites with known ocular dominance and position preference, based on optical-imaging and electrophysiological data. For most targets, multiunit activity was recorded, and receptive fields were plotted, as described above. Latex microspheres (beads) conjugated to either rhodamine (red) or fluoroscein (green) (kindly provided by Dr. L. Katz) were then pressure injected into the cortex at a depth of ~800 μm (cortical layer 4). Typically, the injection sites were <100 μm in diameter in the tangential plane of the cortex and extended from the pial surface into layer V or VI. At some sites, WGA-HRP was iontophoresed into the cortex at a depth of 800 μm by passing 2.5 μA of current for 15 min (with a 7 sec ON/sec OFF cycle)

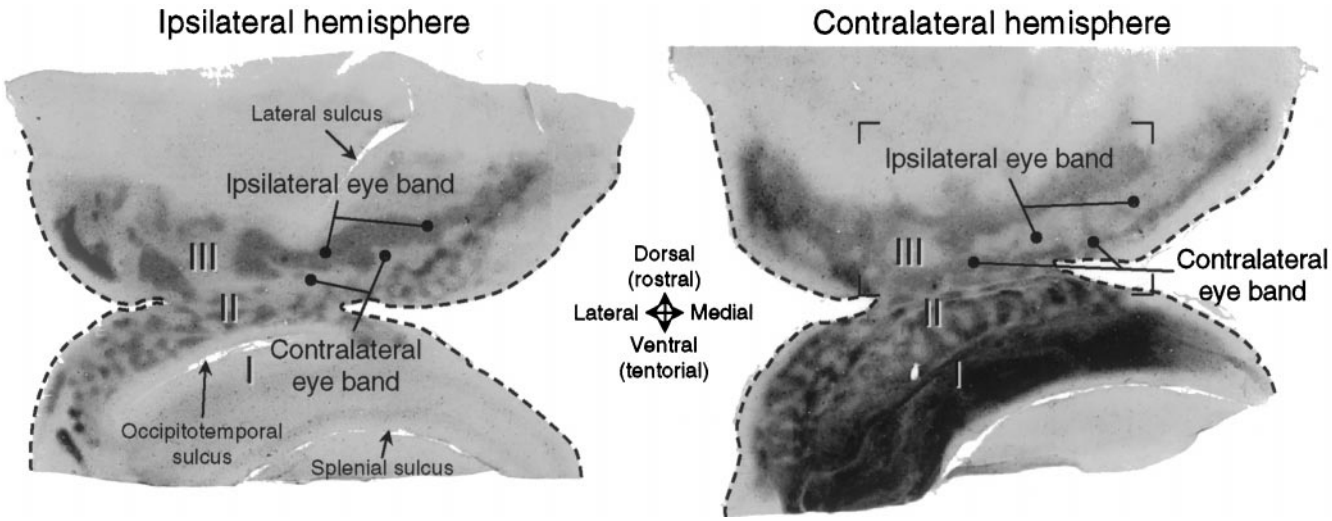

Figure 1. Ocular dominance domains in ferret visual cortex demonstrated by transneuronal transport of WGA-HRP. For each hemisphere, the overall pattern of geniculocortical input was revealed by reconstruction of serial tangential sections obtained from an unfolded and flattened occipital cortex. Unfolding was achieved by making relaxation cuts through the medial and lateral parts of the caudal pole (*dashed lines* on *section edges*). Thus, the dorsal occipital cortex is contained in the *upper leaf* of each *section*, and the ventral (tentorial) side of the occipital lobe is contained in the *lower leaf*, with the middle portion of the caudal pole joining the two. *Dark regions* contain high concentrations of reaction product, indicating zones within which labeled geniculocortical afferents terminate; *ipsilateral* and *contralateral* refer to the side of intraocular injection. To facilitate comparison of patterns in the two hemispheres, the contralateral hemisphere is flipped horizontally to match the ipsilateral hemisphere. The *area framed* by *corners* in the contralateral hemisphere indicates the approximate portion of the hemisphere viewed in optical-imaging experiments. Length of *double-headed arrows*, 1 mm.

through the tip of a glass micropipette containing 5% (w/v) WGA-HRP in normal saline. After a 2–3 d survival period, the ferrets were perfused, and their brains were processed as described above. In addition, the remaining block containing the diencephalon was sectioned at 50 μm in the horizontal plane, which is orthogonal to the orientation of the isoazimuth lines in the topographic map of visual space in the LGN (Zahs and Stryker, 1985). The sections were then mounted onto subbed slides and coverslipped. The position of retrogradely labeled neurons in the thalamus and the outlines of blood vessels and the section edge were digitized using a computer-based *x-y* plotting system (Neurolucida; MicroBrightField, Colchester, VT). After plotting, the coverslips were removed, and the sections were stained with thionin for the demonstration of Nissl substance. The digitized representation of the labeled cells was then displayed over images of the stained sections, using a modified version of NIH Image software.

RESULTS

Ocular dominance domains in ferret visual cortex

Figure 1 illustrates the ocular dominance patterns in both hemispheres of a ferret after intraocular injection and transneuronal transport of WGA-HRP. We recognized three regions in ferret visual cortex that differ in the size, shape, and uniformity of their eye-specific input. First, in the hemisphere contralateral to the injected eye, a broad zone receiving uniform input from the injected eye spans the posterior bank of the splenial sulcus on the tentorial surface of the hemisphere (see Fig. 1, *I*). Presumably, this zone corresponds to the monocular segment of the contralateral visual field, which is viewed exclusively by the contralateral nasal retina. Second, in the caudal pole of both hemispheres, where more central regions of the visual field viewed by both eyes are represented (Law et al., 1988), eye-specific inputs segregate into an interdigitated array of ocular dominance domains (see Fig. 1, *II*). In this part of the map, domains are small (<500 μm in width) and often stripe-like, especially the contralateral eye domains (see Fig. 1, *Contralateral hemisphere*). Third, on the dorsal occipital surface (i.e., in the posterior lateral gyrus), ocular dominance domains are much larger and more irregular in shape (see Fig. 1, *III*). The small contralateral eye domains in the caudal pole merge anteriorly to form a nearly continuous band elongated in the medial-to-lateral axis of the hemisphere. This arrangement is evident in both hemispheres of the case presented but is more obvious in the ipsilateral hemisphere where the unlabeled spaces intercalated between darkly stained ipsilateral eye domains yield to a broad unlabeled zone that extends for ~7 mm across the caudal pole. Immediately anterior to this contralateral eye zone is a second elongated band dominated by input arising from the ipsilateral eye. This succession of elongated contralateral eye and ipsilateral eye bands is most prominent in the medial half of both of these hemispheres, where the lower visual field is represented. In more lateral regions, where the upper visual field is represented, these bands are interrupted as large, irregularly shaped islands of ipsilateral eye input interdigitate with and are surrounded by territory receiving input through the contralateral eye. Finally, there are additional zones labeled via the contralateral eye in the most anterior regions of reactive cortex.

The arrangement of ocular dominance domains was also revealed in a much larger set of animals ($n > 50$) by means of optical imaging of intrinsic signal. These functional representations of ocular preference display all the features described above for anatomical domains revealed by transneuronal transport, although the extent of the imaged ocular dominance map was necessarily much smaller (typically, 4 × 8 mm) and restricted to the dorsal occipital cortex (see Fig. 1, *framed area*). Consequently, most of the cases show the large irregular domains characteristic of the posterior lateral gyrus, with only a limited view of the caudal pole where the small domains are found (it was not possible to expose the tentorial surface and image the monocular segment). A survey of ocular dominance patterns from 10 ferrets reveals considerable interindividual variation in the precise configuration of the domains, especially the large contralateral eye and ipsilateral eye bands (Fig. 2). In agreement with the transneuronal transport demonstration (compare Fig. 1), the ipsilateral eye band may be linear and parallel to the occipital pole (see Fig.

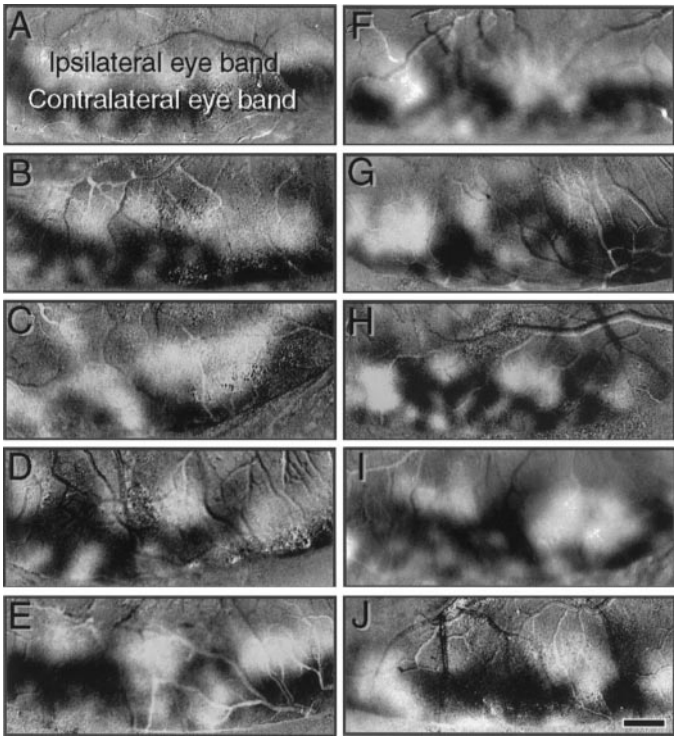

Figure 2. Ocular dominance domains in 10 ferrets (*A–J*) revealed by optical imaging of intrinsic signal. *Dark regions* responded best to a set of gratings presented to the contralateral eye, and *light regions* responded best to the same set of gratings presented to the ipsilateral eye. These and all subsequent *images* are of the left hemisphere, with medial to the *right* and posterior (i.e., the caudal pole of the hemisphere) toward the *bottom*. Note the presence of large ipsilateral eye domains immediately anterior to prominent zones of contralateral eye activity. Scale bar, 1 mm.

2*A–C*), and/or it may be interrupted in one or more places by anterior intrusions of the contralateral eye zone (see Fig. 2*D–J*). Another variation evident both among animals and across the same hemisphere is the rostral-to-caudal extent of the contralateral eye band. In Figure 2*F*, for example, this band narrows to <300 μm in one location and expands abruptly to >1 mm in width just medial to the narrowed segment. Despite these inter- and intraindividual variations, large ipsilateral eye domains were always present anterior to a mostly continuous, although somewhat tortuous, contralateral eye band.

To examine the degree of ocular bias in these large ocular dominance zones, electrophysiological recordings were made from cortical layer 3 (200–500 μm below the pial surface) near the middle of the large ipsilateral eye and contralateral eye domains in 10 ferrets after optical imaging. In each instance, the multiunit activity was strongly biased toward the same eye that preferentially evoked cortical activity during the optical-imaging experiment, and for most sites, the evoked responses were judged to be completely monocular. In four ferrets, the responses to stimulation of each eye were analyzed quantitatively, and an ocular dominance index was computed. The mean index ($\pm$ SD) obtained from the large contralateral eye domains was $+0.96 \pm 0.06$ (eight sites), and the corresponding value from the large ipsilateral eye domains was -0.89 ± 0.10 (eight sites). Thus, even in upper cortical layers, there was little or no input from the nonpreferred eye to the large ocular dominance domains.

Finally, anterior to the large ipsilateral eye domains, the rostral contralateral eye zone that appears prominent in the transneuronal material was considerably less conspicuous in the optical-imaging experiments (compare Figs. 1, 2). In some cases, a hint of contralateral eye preference is present just anterior to the ipsilateral eye band (see Fig. 2*B*,*C*), but in none of the experiments did it approach the intensity of the signal in the other, more posterior regions of the cortex.

Location of a reversal in the map of visual space

One interpretation of these variations in the ocular dominance pattern is that the cortical regions occupied by small and large domains are distinct visual areas. In this conception, the small domains in the caudal pole define the extent of V1, and the more anterior region occupied by large, irregular domains correspond to V2 and/or additional visual areas (see also Redies et al., 1990). Thus, the V1–V2 border would coincide with the posterior limit of the large contralateral eye band (i.e., where small contralateral eye domains merge anteriorly into an elongated zone). To test this interpretation of the ocular dominance pattern, we assessed the representation of visual space in the same cortical region that was imaged for ocular dominance. Our rationale is based on the fact that in all mammals examined, the orderly maps of visual space in V1 and V2 are arranged in an approximately mirror-symmetric manner (Van Essen, 1979; Kaas and Krubitzer, 1991). The border between these two visual areas, therefore, corresponds to a reversal in the progression of receptive field locations that characterize each map. We used optical imaging to record intrinsic signals evoked by a series of spatially restricted stimuli from the peripheral contralateral visual field (+20 or 25°) to at least 10° into the ipsilateral visual field (see Materials and Methods). Our expectation, based on an earlier study (Law et al., 1988), was to record optical responses in the form of bands of activity elongated in the medial-to-lateral axis that would translate systematically across the visual cortex. One continuous band of activity in V1 should progress from posterior to anterior, and a second band in V2 should shift in the opposite direction as the stimulus moved from the peripheral part of the contralateral visual field toward the vertical meridian. The results from such an experiment for stimuli centered 10° on either side of the vertical meridian are shown in Figure 3.

The presentation of a single 5°-wide vertical stimulus centered 10° into the contralateral field produced two distinct regions of activation in the anterior part of the imaged cortex (see Fig. 3*A*,*B*). As the stimulus was moved toward the vertical meridian, the location of both activated regions shifted posteriorly in the cortex (compare Fig. 3*C–F*). In addition, another band of activity elongated in the medial-to-lateral axis of the cortex emerged from the posterior limit of the imaging field (see Fig. 3*C*,*D*) and progressed in the anterior direction (compare Fig. 3*C–J*). With the stimulus centered on the vertical meridian, the posterior-shifting regions of activation and the anterior-shifting band of signal appeared to merge along the posterior boundary of the large ipsilateral eye domains (see Fig. 3*E*,*F*). Thus, the posterior progression of the locus of activity, which began with the stimulus positioned 20° into the contralateral field (the first two positions are not shown), terminated when the stimulus was centered on the vertical meridian. However, as the stimulus was centered at positions up to 10° across the vertical meridian in the ipsilateral visual field, the anterior-shifting band of activation continued its rostral progression but separated into several distinct regions of activity (see Fig. 3*G–J*). The systematic progression of evoked cortical activity evident in Figure 3*A–J* and the relation of the map of visual space to the ocular dominance domains are best

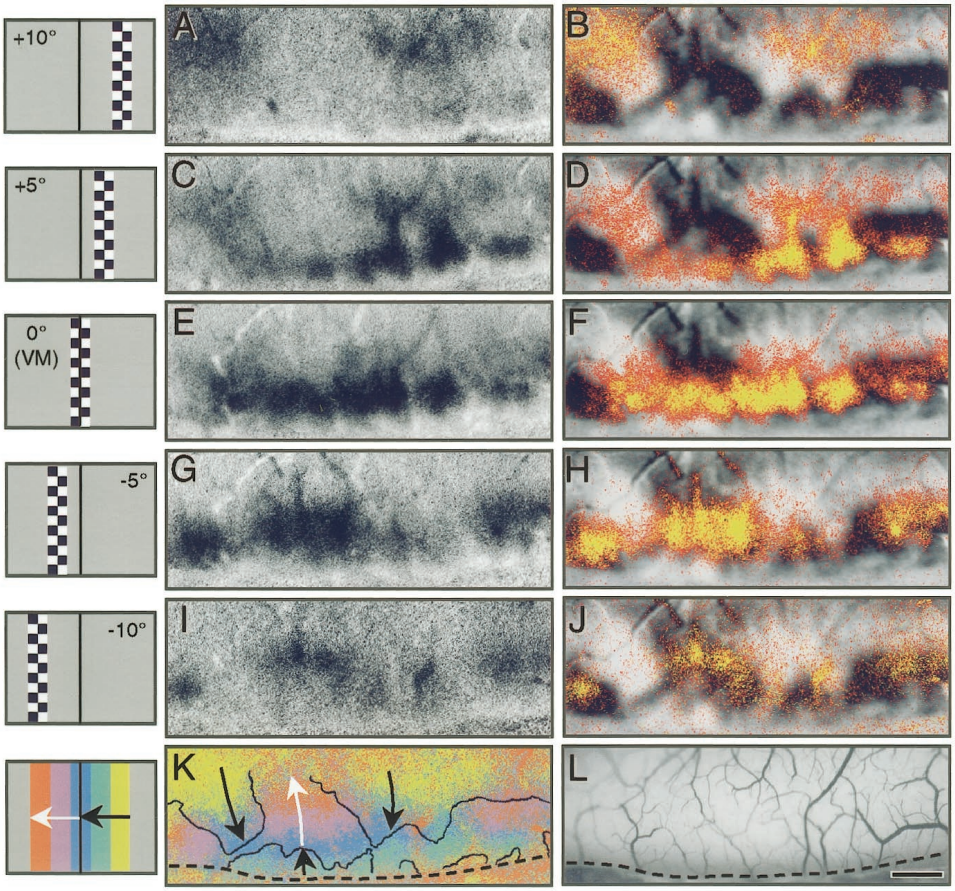

Figure 3. Organization of the map of visual space revealed by optical imaging of intrinsic signal. *A–J*, A counterphasing checkerboard pattern 5° in width and 60° in height was centered at each of five positions, from 10° into the contralateral visual field (positive azimuths) to 10° into the ipsilateral visual field (negative azimuths). *A*, *C*, *E*, *G*, *I*, The pattern of cortical activation in response to each of the stimulus positions indicated to the *left*. *B*, *D*, *F*, *H*, *J*, The same activation patterns displayed over the map of ocular dominance for this ferret, which is shown in Figure 2*F*. All pixels from the native topography data images with *gray* levels >190 (range, 0–255) were selected and colored *red*, except for the saturated pixels (level 255) that were colored *yellow*; for clarity, pixels with *gray* values <190 are not displayed. This same set of data in *B*, *D*, *F*, *H*, and *J* may be viewed as an animation at http://www.jneurosci.org; the interdigitation of the reversed maps of visual space is best appreciated when the animation sequence is looped back and forth or when each frame is advanced manually. *K*, A position preference map in which the color code represents the stimulus position that produced the greatest activation for every pixel in the imaged cortical field. The *solid black line* indicates the boundary between the large ocular dominance domains, and the *dashed black line* indicates the caudal edge of the cortex (also in the vascular image of this same cortical exposure in *L*). The *arrows* in *K* and its legend (on the *left*) serve to emphasize the progressive representation of visual space and its reversal along the boundary between the large ocular dominance domains (compare *A*, *C*, *E*, *G*, *I*). Scale bar, 1 mm. VM, Vertical meridian.

appreciated by viewing an animation of these data in topographic sequence. Interested readers may view an animation of Figure 3, *B, D, F, H,* and *J,* at http://www.jneurosci.org.

The overall organization of the map of visual space may also be appreciated by computing a position preference map (see Fig. 3*K*). This representation of the data reveals the presence of two systematic maps of visual space, one in the caudal pole (i.e., V1) and a second "reversed" map in the more rostral portions of the posterior lateral gyrus (i.e., V2). The caudal map was extended continuously over the region of cortex that included both the small ocular dominance domains and the large contralateral eye band, whereas the reversed representation was precisely contained within the large ipsilateral eye domains (see Fig. 3*K*). The reversal in the map of visual space occurred not at the junction between small and large ocular dominance domains but along the boundary between the large contralateral eye band and the large, anterior ipsilateral eye domains.

An ipsilateral visual field representation in V1

As illustrated in Figure 3, the large, contralateral eye ocular dominance zone at the anterior margin of V1 contains an extension of the visuotopic map beyond the vertical meridian to ~10° into the ipsilateral visual field. The correspondence between this domain and the ipsilateral visual field is especially clear in regions where the large contralateral eye and ipsilateral eye domains interdigitate (see, for example, the *left portion* of the *panels* in Fig. 3 and the accompanying animation). In these regions, the representation of the ipsilateral visual field is confined to the large contralateral eye zone and is virtually absent from the adjacent large ipsilateral eye domain, which contains a reversed map of the contralateral visual field.

To confirm these observations, we mapped the receptive fields of sites in cortical layer 3 by electrophysiological means in 10 ferrets after optical imaging of ocular dominance patterns. Figure 4 illustrates a case in which two series of recordings were made at two medial-to-lateral levels that traversed the large ocular dominance bands in the posterior lateral gyrus. The most caudal recording sites in both penetrations showed receptive fields that were centered in the contralateral field within 6° of the vertical meridian. Recording sites within the elongated contralateral eye band, however, were centered across the vertical meridian in the ipsilateral visual field. Indeed, the representation of the vertical meridian lay at the posterior boundary of this contralateral eye band, as indicated by the receptive field centers from sites that straddled this ocular dominance boundary. Sites within the contralateral eye band typically displayed receptive fields that extended as much as 15° into the ipsilateral visual field [consistent with Law et al. (1988), their Fig. 2]. Although our analysis was not exhaustive, we did not detect any unusual difference in the size or structure of receptive fields in this zone, in comparison with adjacent parts of V1 that represent the contralateral visual field. Recording sites rostral to the contralateral eye band were centered back in the contralateral visual field, indicating that the reversal in the map of visual space occurred at the boundary between the contralateral eye and ipsilateral eye bands.

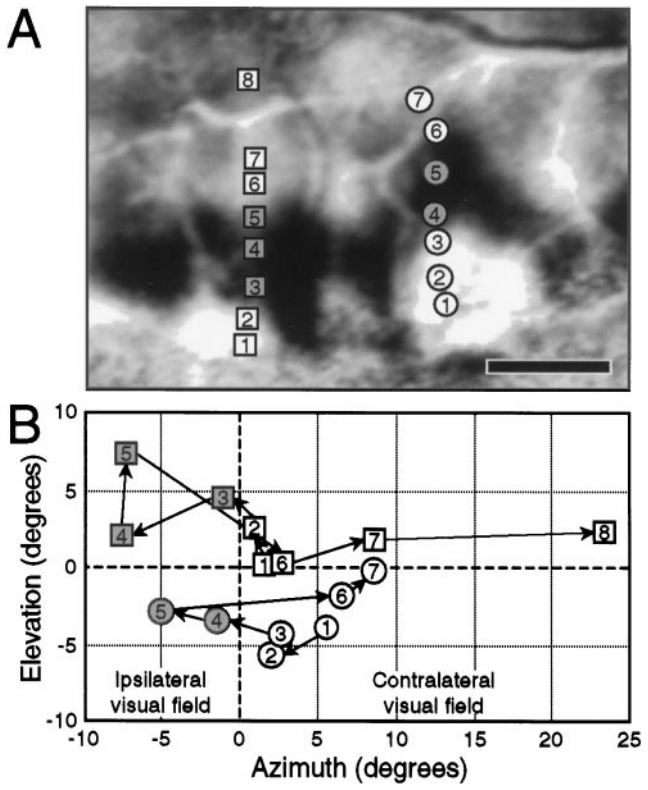

Figure 4. Organization of the map of visual space revealed by electrophysiological recording. *A*, Two parallel series of sites (*squares labeled 1–8* and *circles labeled 1–7*) were sampled by orthogonal electrode penetration. The rostral-to-caudal path of each series was chosen to be approximately parallel to isoelevation lines and orthogonal to isoazimuth lines in the cortical map of visual space, as well as to traverse the large ocular dominance bands in this region. *B*, The plot of receptive field centers for cortical sites from which multiunit activity was recorded indicates that the extended contralateral eye band harbors a visuotopic representation of the central ipsilateral visual field (*shaded symbols*). Significant discontinuities in the mapping of visual space are evident at the border between the large contralateral eye and ipsilateral eye domains. Receptive field centers abruptly shift back from the ipsilateral to the contralateral visual field with continued rostral progression in the cortex. Note the jump in visual space between both pairs of sites labeled *5* and *6*. Scale bar, 1 mm.

Topographic discontinuity along the V1–V2 border

The juxtaposition of an ipsilateral visual field representation in V1 and a contralateral visual field representation in V2 mandates a sizeable discontinuity in the mapping of visual space along their border. Results from both optical-imaging and multiunit-recording experiments confirm the presence of such a discontinuity. Across regions where the large contralateral eye and ipsilateral eye domains form parallel bands, there are consistent jumps of position preference from 10 to 15° into the ipsilateral visual field to positions in the contralateral visual field near the vertical meridian. In the case presented in Figure 4, for example, the centers of the receptive fields recorded from the two pairs of consecutive sites (300 μm apart) very near this ocular dominance boundary were separated by >9° of visual space (Fig. 4, *symbols* 5, 6). This discontinuity is especially prominent in cases where the large ipsilateral eye and contralateral eye domains interdigitate. Because the visuotopic maps in such regions are organized in opposite directions in the cortex, sites that lie in the most rostral part of a contralateral eye domain, at the furthest extent of the ipsilateral visual field representation, are juxtaposed to sites in the ipsilateral eye domain whose receptive fields are located well into the contralateral visual field (see Figs. 3*K*, 5*A*,*B*). The topographic discontinuity is least in regions where the large contralateral eye domain is markedly diminished or absent. Such a region is present in the *left side* of the imaged cortical field illustrated in Figure 3. Along the interface of the narrowed segment of the contralateral eye band and the large ipsilateral eye domain, the topographic discontinuity is minimal or nonexistent; the map of visual space simply reverses with little or no disruption. However, along the medial and lateral boundaries of this large ipsilateral eye domain, the discontinuity is significant (this is especially evident in the animation). Thus, the degree of topographic discontinuity varies markedly along the V1–V2 border, in accord with the size of the contralateral eye band and the extent of its interdigitation with the large ipsilateral eye domains.

In principle, misalignment of the two eyes could produce an apparent representation of the ipsilateral visual field and a discontinuity in visual field mapping at the boundary between ocular dominance domains. However, this cannot explain the results that we have presented. The slight divergence of the optic axes seen in each animal tested is exactly the opposite of what would be needed to induce an ipsilateral visual field representation artifactually. Indeed, because we did not correct for these misalignments, our estimates of the extent of the ipsilateral visual field representation in V1, as well as the magnitude of the visuotopic discontinuity across the ocular dominance boundary, are conservative. Finally, the arrangement of LGN inputs to the V1–V2 border region (see below) supports both the direction and extent of topographic displacement that we demonstrated with physiological techniques.

The arrangement of LGN inputs to the V1–V2 border region

Taken together, these results suggest an ocular-specific arrangement of LGN inputs to the V1–V2 border region in the ferret, with LGN relay cells driven solely by the contralateral eye terminating on the V1 side of the border and those driven by the ipsilateral eye terminating on the V2 side of the border. Furthermore, in regions where the V1 and V2 representations are interdigitated, sites on either side of this boundary should receive their inputs from LGN neurons that lie in topographically disparate parts of the nucleus. To test these predictions, small injections of retrograde axonal tracers were placed into the large contralateral eye and ipsilateral eye domains defined by optical imaging. In the experiment illustrated in Figure 5, a large ipsilateral eye domain was injected with fluoroscein-conjugated latex microspheres (green beads), and contralateral eye regions that flanked the ipsilateral eye domain laterally and medially were injected with rhodamine-conjugated latex microspheres (red beads). Two injections of red beads were made to insure that retrogradely labeled cells would be present in the same horizontal sections through the LGN [i.e., along the same isoelevation lines (see Zahs and Stryker, 1985)]. The green bead injection produced a dense cluster of retrogradely labeled neurons restricted to lamina A1, which receives input exclusively from the ipsilateral eye (see Fig. 5*C*). In contrast, the red bead injections resulted in a single cluster of labeled neurons found along the medial edge of lamina A, which receives input exclusively from the contralateral eye. In addition, a sparse stream of labeled cells extended posteriorly around the medial edge of lamina A1 (i.e., embedded within and medial to the lamella that encapsulates lamina A1) toward lamina C (see Fig. 5*C*). The continuity of this stream of cells with lamina

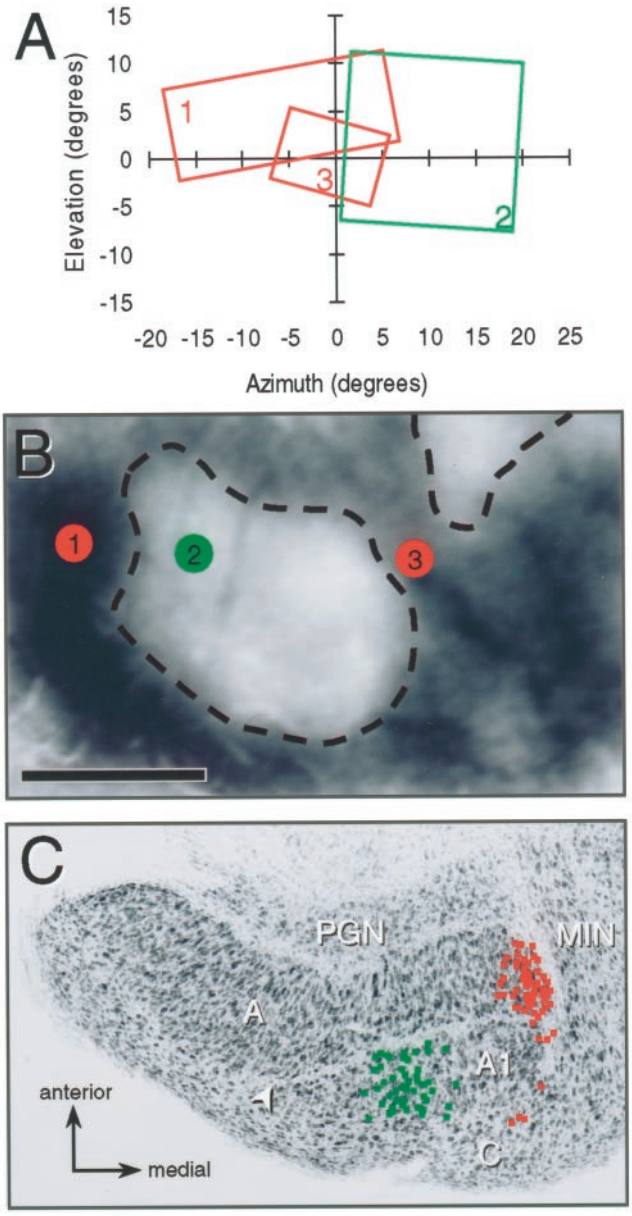

Figure 5. Source of geniculate input to the V1–V2 border region. After optical imaging of the visual cortex to reveal ocular dominance domains and the map of visual space, sites were selected for injection of retrograde axonal tracers. *A*, Before injection, the aggregate receptive fields of each *site* were plotted to confirm that the representations at *sites 1* and *3* were driven exclusively by the contralateral eye and extended into the ipsilateral visual field and that the receptive field at *site 2* was exclusively driven by the ipsilateral eye and confined to the contralateral visual field. *B*, Injections of *red* beads were placed in cortical layer IV at sites 1 and 3, both of which were in contralateral eye domains; a similar injection of *green* beads was placed at site 2 in a large ipsilateral eye domain. *C*, The pattern of retrograde label in a single horizontal section through the LGN is shown; lamina A and A1 are the principal targets of the crossed and uncrossed retinal projections, respectively. Each *green* and *red symbol* marks the position of a single neuron retrogradely labeled with *green* or *red* beads plotted over the same section counterstained to demonstrate Nissl substance. *Dashed lines* in *B* outline the large ipsilateral eye domains, and the *arrowhead* in *C* marks the lateral edge of lamina A1. *PGN*, Perigeniculate nucleus; *MIN*, medial interlaminar nucleus. Scale bars: *B,* 1 mm; *arrow* length in *C*, 250 μm.

A and the fact that cells in this position are only labeled by injections that involve the ipsilateral visual field representation suggest that they are driven by the contralateral eye. A contralateral eye input to cells between lamina A1 and the medial interlaminar nucleus is supported by studies of the termination patterns of retinogeniculate input that show a projection from the contralateral eye that encompasses the medial edge of lamina A1 [e.g., see Linden et al. (1981), their Fig. 3]. These results, together with similar findings from four additional cases with V2 injections and three additional ferrets with comparable V1 injections, confirm the strict monocularity of these central representations in the V1–V2 border region. Furthermore, these experiments also demonstrate that the principal geniculate input to the representation of the ipsilateral visual field in V1 derives from neurons along the most medial edge of lamina A. Thus, the ipsilateral visual field representation in V1 does not result from the insertion of a distinct set of thalamic inputs, such as from the medial interlaminar nucleus (see, e.g., Lee et al., 1984; Payne, 1990); it merely reflects the complete cortical mapping of LGN lamina A, including its caudal–medial extension. Finally, the disparate location of the red bead– and green bead–labeled cells along the medial-to-lateral axis of the nucleus also shows that the complex visuotopy of the V1–V2 border is entirely consistent with the spatial arrangement of LGN afferents.

LGN inputs to the rostral contralateral eye zone

Our data suggest that V2 in ferret is comprised of the large ipsilateral eye domains. However, the contralateral eye zones that lie rostral to these domains (see Fig. 1) could, in principle, constitute the contralateral eye's input to V2. If this were so, we would expect this zone to receive a matching projection from LGN lamina A to compliment the inputs from lamina A1 that terminate in the large ipsilateral eye domains. To investigate this possibility, we made injections of retrograde tracers into the rostral contralateral eye zones in two ferrets. In both cases, injection of retrograde tracers into the rostral contralateral eye zones produced a dense cluster of retrogradely labeled neurons in lamina C (Fig. 6), with no labeled neurons in lamina A. This pattern of label implies that the rostral contralateral eye zones are not simply the contralateral eye's counterpart of the large ipsilateral eye domains in V2. This interpretation is further supported by the observation that the optical-imaging techniques that were effective at revealing visual activation in the large ipsilateral eye domains were primarily ineffective for these rostral contralateral eye zones. Moreover, several electrophysiological penetrations in the rostral contralateral eye zones revealed, at best, only weak evoked responses that were difficult to characterize (the best responses were evoked by large flashing stimuli rather than the drifting gratings that were optimal for V1 and V2). The differential responsiveness of these domains and the anatomical data presented in Figures 5 and 6 are consistent with the character of the evoked responses recorded previously in the LGN (Zahs and Stryker, 1985). In that report, evoked activity in lamina C was described as transient and Y-like, whereas responses in the laminae A and A1 were "extremely tonic" and X-like. Taken together, these observations indicate that the rostral contralateral eye zones are not part of V2 and may constitute an additional visual area.

DISCUSSION

We have demonstrated a systematic relationship between an unusual system of ocular dominance domains and maps of visual

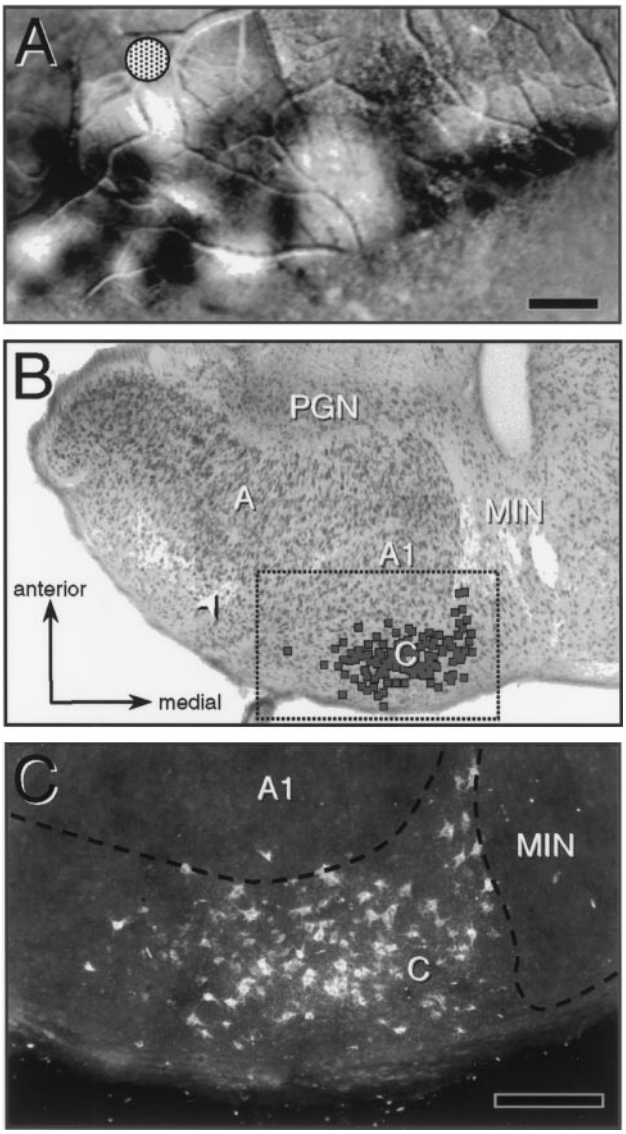

Figure 6. Source of geniculate input to the rostral contralateral eye zone. *A*, After optical imaging of the visual cortex to reveal ocular dominance domains, a contralateral eye site rostral to the large ipsilateral eye domains was selected for injection of WGA-HRP. The *stippled circular region* in *A* marks the *location* and *size* of the cortical injection. *B, C*, In the LGN, retrogradely labeled neurons were primarily confined to the medial portion of lamina C; each *symbol* in *B* marks a labeled neuron. An occasional labeled cell was found in neighboring regions of lamina A1, presumably as a result of the encroachment of the injection site into the ipsilateral eye domain. *C,* A photomicrograph shows the *boxed portion* of *B* viewed under dark-field illumination. Scale bars: *A*, 1 mm; *arrow* length in *B*, 500 μm; *C*, 250 μm.

space in ferret visual cortex. The exceptionally large and irregular domains in this species include portions of V1, all of V2, and an additional zone rostral to V2 (summarized schematically in Fig. 7). Our results indicate that the large domains in V1 and V2 harbor monocular representations of visual space that lack matching geniculate inputs driven by the other eye. The large contralateral eye band in the caudal part of the dorsal occipital cortex is the representation of the ipsilateral visual field in V1, and the large ipsilateral eye domains that lie just rostral to V1 constitute the representation of the contralateral visual field in V2. In the discussion that follows, we relate these findings to observations in other species, including hypopigmented carnivores, and consider the factors that may account for this pattern.

A central monocular segment in V1

We have demonstrated a large contralateral eye ocular dominance band near the rostral boundary of V1 that extends the representation of visual space beyond the vertical meridian for as much as 15° into the ipsilateral visual field. Because of the ocularity of this zone and the region of visual space it represents, visual input to this zone must derive chiefly from the contralateral temporal retina. Previous studies of the retinogeniculate projection in ferret are consistent with this interpretation. The uncrossed projection to the LGN arises from ganglion cells that are strictly confined to the temporal segment of the retina. In contrast, the crossed projection arises from ganglion cells that occupy the entire nasal retina and extend nearly to the temporal margin of the retina (Vitek et al., 1985; Morgan et al., 1987; Cucchiaro, 1991; Wingate et al., 1992; Baker and Reese, 1993; Thompson and Morgan, 1993; FitzGibbon et al., 1996). As a result of this encroachment into the temporal retina, the crossed projection conveys information from the central portion of the ipsilateral visual field that is not represented in the uncrossed pathway (see Fig. 7). In this sense, the large contralateral eye band at the rostral border of V1 is analogous to the larger contralateral eye zone that defines the monocular crescent representation in the ventral (peripheral) part of V1. Both reflect a mismatch in the extent of visual space represented in the crossed and uncrossed pathways, and both receive their inputs from regions of LGN lamina A that have no counterpart in lamina A1. For these reasons, we find it useful to consider this ipsilateral visual field representation a "central monocular segment."

The ferret is not unique in either the presence of an ipsilateral visual field representation within V1 or the corresponding asymmetry in the pattern of ganglion cell decussation. Ipsilateral visual field representations have been reported for cat (Payne, 1990; Payne and Siwek, 1991), tree shrew (Bosking et al., 1998), sheep (Pettigrew et al., 1984), rabbit (Hughes and Vaney, 1982), and opossum (Volchan et al., 1988). In cat (Cooper and Pettigrew, 1979a; Illing and Wässle, 1981) and goat (Pettigrew et al., 1984), a corresponding asymmetrical pattern of retinal decussation has also been described. It is, therefore, surprising that with the possible exception of one report in the sheep (Pettigrew et al., 1984), there is little evidence in other species for the presence of a large contralateral eye domain near the V1–V2 border, similar to what we report here. Studies of the ipsilateral visual field representation in the "transition zone" between V1 and V2 of cat, however, indicate that cells are dominated by input from the contralateral eye (Whitteridge and Clarke, 1982; Pettigrew and Dreher, 1987). Perhaps a more thorough analysis of the relation between the map of visual space and the pattern of ocular dominance domains in other species will reveal a common plan. Alternatively, LGN afferents representing the ipsilateral visual field could terminate within the contralateral eye zones of a homogeneous pattern of small, interdigitated ocular dominance domains. Whatever the arrangement in other species, our results emphasize that the mismatch in the extent of the crossed and uncrossed pathways is likely to be a significant factor in shaping the functional architecture of the V1–V2 border region in many mammals.

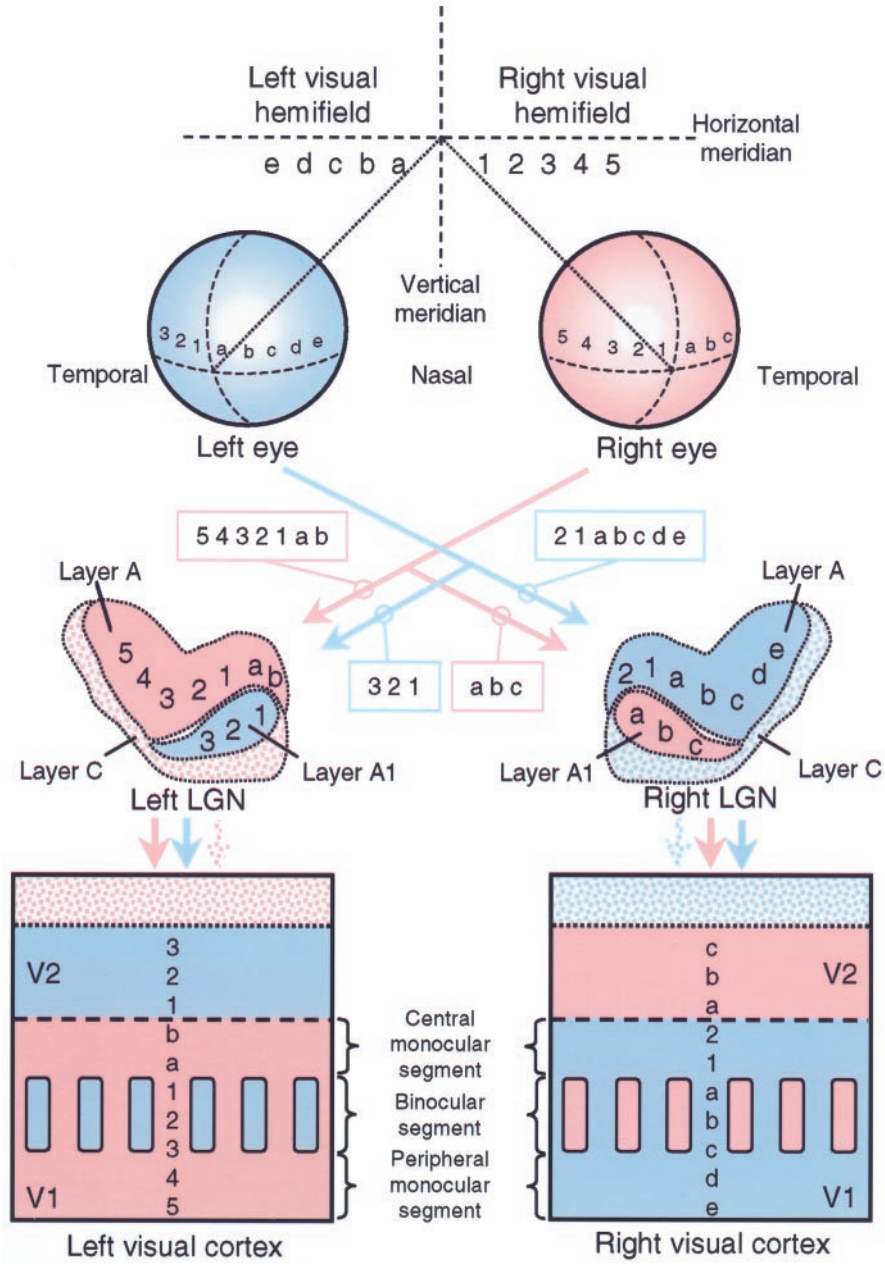

Figure 7. Summary of the representation of visual space in the ferret visual system. The contralateral visual field is seen by the nasal division of each retina, and the ipsilateral visual field is viewed by the temporal division. The central projections of the crossed and uncrossed pathways that arise from these divisions, however, are asymmetric. The crossed projection includes the axons of certain ganglion cells in the temporal retina, in addition to the axons of virtually all ganglion cells in the nasal retina. In contrast, the uncrossed projection arises exclusively from ganglion cells in the temporal division. Thus, the crossed projection conveys information from the central portion of the ipsilateral visual field that is not present in the uncrossed pathway. The crossed projection terminates in the LGN mainly in laminae A and C, with the ipsilateral visual field representation mapped along the medial edge of lamina A. The uncrossed projection innervates lamina A1. For simplicity, the uncrossed projection to the C sublaminae and both crossed and uncrossed projections to the medial interlaminar nucleus are not illustrated. In the visual cortex, V1 is comprised of distinct regions that differ in the distribution of geniculate afferents and in the portions of visual space represented in each. Anterior to V1 is a second, reversed representation of the contralateral visual field in V2, which is comprised of large domains driven by the ipsilateral eye. Significant discontinuities in the mapping of visual space occur along the V1–V2 border (shown as a *straight horizontal dashed line* for simplicity); note the *sequence* of *numbers* and *letters* on *either side* of the *border*. Finally, anterior to V2 there is another type of large ocular dominance zone that is driven by the contralateral eye. This rostral zone receives geniculate input from lamina C and may constitute an additional visual area.

A monocular V2 representation

Another remarkable feature of the ferret visual cortex is the presence of the large ipsilateral eye ocular dominance domains lying just rostral to V1. Our results suggest that these domains constitute a single representation of the central 20–25° of the contralateral visual field, which is broken up in some regions by anterior incursions of V1. In all mammals that have been studied, the cortical area that lies immediately rostral to V1 exhibits a reversed topographic order, with respect to V1 (Van Essen, 1979; Kaas and Krubitzer, 1991). In this regard, the ferret is no exception. However, our results indicate that V2 in the ferret, unlike that in other species, receives its principal input from LGN afferents that are driven by the ipsilateral eye, with no counterpart supplied by the contralateral eye. One plausible explanation of this finding is that the strictly monocular V2 representation, like the ipsilateral visual field representation in V1, might derive from asymmetries in the organization of retinal ganglion cells that give rise to crossed and uncrossed central pathways. In this conception, visual input to V2 arises from a distinct class of ganglion cells whose distribution is restricted to the temporal retina. This possibility has yet to be examined explicitly; however, studies of retinal ganglion cell morphology in the ferret provide support for asymmetries in the classes of ganglion cells that contribute to the crossed and uncrossed projections (Vitek et al., 1985; Wingate et al., 1992; FitzGibbon et al., 1996). Furthermore, if this hypothesis is correct, then one would expect that the LGN inputs to V2 would arise from a class of relay cells in lamina A1 that are different from those that supply the small, ipsilateral eye domains in V1, which have a counterpart in the nasal retina. The distinctiveness of the LGN input to V2 is consistent with the results of single-unit recordings showing that neurons in V2 of the ferret have larger receptive fields and respond better to fast-moving

stimuli than do those in V1 (Law et al., 1988). It is also supported by double-label experiments that indicate that very few neurons in lamina A1 project to both V1 and V2 (White et al., 1998).

Relation to hypopigmented carnivores

Our findings accord with previous studies in albino and hypopigmented animals showing that patterns of ganglion cell decussation have significant consequences for both cortical and subcortical architecture (Guillery and Kaas, 1971; Hubel and Wiesel, 1971; Kaas and Guillery, 1973; Shatz, 1977; Cooper and Pettigrew, 1979b; Ault et al., 1995). In these abnormal animals, ganglion cells from the temporal retina are misrouted to the contralateral thalamus, resulting in a significantly enlarged representation of the ipsilateral visual field in the A layers of the LGN and along the V1–V2 border. A similarly expanded representation of the ipsilateral visual field may be induced in normally pigmented cats by unilateral section of the optic tract, a manipulation that promotes the maintenance of an exuberant crossed projection from the temporal retina to the LGN (Schall et al., 1988). This expansion of the ipsilateral visual field representation, in hypopigmented strains at least, is accompanied by a profound reduction in the size and central representation of the uncrossed retinal projection. It could be argued that the enlarged ipsilateral visual field representation requires the loss of this uncrossed input and the occupation of the normal target zones in lamina A1 by inputs from the contralateral temporal retina. However, studies of the retina in normally pigmented ferrets, including heterozygous ferrets that carried one albino gene, showed no obvious deficiency in the ipsilateral projections of the temporal retina (Morgan et al., 1987; Cucchiaro, 1991; Thompson et al., 1991; Thompson and Morgan, 1993). In addition, we found no disruption or reduction of the normal cytoarchitecture of LGN lamina A1 (White et al., 1998). Moreover, the robust representation of inputs derived from the ipsilateral eye in both V1 and V2 attests to the efficacy of the uncrossed retinal pathway. Thus, the presence of significant ipsilateral visual field representation in ferret and, presumably, other normally pigmented species need not come at the expense of normal representation of the ipsilateral temporal retina.

A complex V1–V2 boundary

Perhaps the most striking aspect of our data is the visuotopic and morphological complexity of the border between V1 and V2. The marked discontinuity in the mapping of visual space that occurs at this boundary—like the monocular representations in V1 and V2—is explained by the asymmetrical decussation of ganglion cells in the nasal and temporal segments of the retina. As discussed above, there is very little or no input from the ipsilateral visual field supplied by the uncrossed retinal projection. Consequently, the representation of visual space contained within the ipsilateral eye ocular dominance domains in V2 must be restricted to the contralateral visual field. Because these domains border and interdigitate with contralateral eye domains in V1 that represent the ipsilateral visual field, a sizable discontinuity in the mapping of visual space is inevitable across their boundary.

A finding that is more difficult to understand is the irregular shape and interindividual variation of the border between V1 and V2. This was unexpected because of previous studies in the ferret (Law et al., 1988), as well as in a variety of other species, in which the V1–V2 border has been depicted as a relatively straight line. In many species, especially primates, the physiologically defined border (line of reversal in the visuotopic map) is correlated with a striking difference in cytoarchitecture between Brodmann's areas 17 and 18 and provides strong confirmation of the linear nature of this boundary. Although previous studies of ferret visual cortex have identified an area 17–18 boundary based on cytoarchitectonic criteria (Rockland, 1985; Law et al., 1988), it is much less distinct than that of primates. Moreover, it is not clear whether it corresponds to the V1–V2 border defined physiologically. In either case, V1 and V2 in the ferret may be similar to many functional representations in the extrastriate cortex of primates and cats that lack conspicuous cytoarchitectural borders (Rosenquist, 1985; Van Essen, 1985; Rosa, 1997). Indeed, certain complexities of the V2–V3 border region in cat identified by electrophysiological analyses, including striking differences among individuals (Donaldson and Whitteridge, 1977; Tusa et al., 1979; Albus and Beckmann, 1980), bear some resemblance to the fractionation of V2 and the irregularity of the V1–V2 border in ferret. Because nonlinear boundaries of the sort we have demonstrated in the ferret are more difficult to appreciate using standard electrophysiological sampling methods, it is likely that the irregularity of other areal boundaries has been underestimated.

Conclusion

These findings have demonstrated regional variations in the arrangement of ocular dominance domains and their systematic relation to monocular, topographic representations of central visual space. The ferret represents a departure from the conventional view, based mainly on studies of cat and macaque, that the binocular visual field is necessarily represented in visual cortex by matching inputs from the two eyes. This conclusion implies that for the ipsilateral visual field representation in V1 and for all of V2, neural computations based on binocular integration of geniculate inputs are not possible. Although the significance of this architecture for visual function is uncertain, the exceptional organization of ferret visual cortex need not imply deviations from the fundamental principles of neural development that have been established in the visual cortex of other species (Purves and Lichtman, 1985; Daw, 1995). Rather, our analysis indicates that the most proximal cause of the unusual features of the ferret visual cortex is likely to reside at the level of the retina, in the distribution and decussation patterns of retinal ganglion cells.

REFERENCES

Albus K, Beckmann R (1980) Second and third visual areas of the cat: interindividual variability in retinotopic arrangement and cortical location. J Physiol (Lond) 299:247–276.

Anderson PA, Olavarria J, Van Sluyters RC (1988) The overall pattern of ocular dominance bands in cat visual cortex. J Neurosci 8:2183–2200.

Ault SJ, Leventhal AG, Vitek DJ, Creel DJ (1995) Abnormal ipsilateral visual field representation in areas 17 and 18 of hypopigmented cats. J Comp Neurol 354:181–192.

Baker GE, Reese BE (1993) Chiasmatic course of temporal retinal axons in the developing ferret. J Comp Neurol 330:95–104.

Bonhoeffer T, Grinvald A (1996) Optical imaging based on intrinsic signals: the methodology. In: Brain mapping: the methods (Toga AW, Mazziotta JC, eds), pp 55–97. San Diego: Academic.

Bosking WH, Kretz R, Fitzpatrick D (1998) Ipsilateral visual field representation and visuotopic specificity of callosal connections in tree shrew striate cortex. Soc Neurosci Abstr 24:1755.

Cooper ML, Pettigrew JD (1979a) The decussation of the retinothalamic pathway in the cat, with a note on the major meridians of the cat's eye. J Comp Neurol 187:285–312.

Cooper ML, Pettigrew JD (1979b) The retinothalamic pathway in Siamese cats. J Comp Neurol 187:313–348.

Cucchiaro JB (1991) Early development of the retinal line of decussation in normal and albino ferrets. J Comp Neurol 312:193–206.

Daw NW (1995) Visual development. New York: Plenum.

Donaldson IML, Whitteridge D (1977) The nature of the boundary

between cortical visual areas II and III in the cat. Proc R Soc Lond [Biol] 199:445–462.

Durbin R, Mitchison G (1990) A dimension reduction framework for understanding cortical maps. Nature 343:644–647.

Erwin E, Miller KD (1998) Correlation-based development of ocularly matched orientation and ocular dominance maps: determination of required input activities. J Neurosci 18:9870–9895.

FitzGibbon T, Wingate RJ, Thompson ID (1996) Soma and axon diameter distributions and central projections of ferret retinal ganglion cells. Vis Neurosci 13:773–786.

Guillery RW, Kaas JH (1971) A study of normal and congenitally abnormal retinogeniculate projections in cats. J Comp Neurol 143:73–100.

Horton JC, Hocking DR (1996) Intrinsic variability of ocular dominance column periodicity in normal macaque monkeys. J Neurosci 16:7228–7239.

Hubel DH, Wiesel TN (1971) Aberrant visual projections in the Siamese cat. J Physiol (Lond) 218:33–62.

Hubel DH, Wiesel TN (1977) Functional architecture of macaque visual cortex. Proc R Soc Lond [Biol] 198:1–59.

Hughes A, Vaney DI (1982) The organization of binocular cortex in the primary visual area of the rabbit. J Comp Neurol 204:151–164.

Illing R-B, Wässle H (1981) The retinal projection to the thalamus in the cat: a quantitative investigation and a comparison with the retinotectal pathway. J Comp Neurol 202:265–285.

Kaas JH, Guillery RW (1973) The transfer of abnormal visual field representations from the dorsal lateral geniculate nucleus to the visual cortex in Siamese cats. Brain Res 59:61–95.

Kaas JH, Krubitzer LA (1991) The organization of extrastriate visual cortex. In: Vision and visual dysfunction, Vol 3, Neuroanatomy of the visual pathways and their development (Dreher B, Robinson SR, eds), pp 302–323. London: Macmillan.

Law MI, Zahs KR, Stryker MP (1988) Organization of primary visual cortex (area 17) in the ferret. J Comp Neurol 278:157–180.

Lee C, Malpeli JG, Schwark HD, Weyand TG (1984) Cat medial interlaminar nucleus: retinotopy, relation to tapetum, and implications for scotopic vision. J Neurophysiol 52:848–869.

Linden DC, Guillery RW, Cucchiaro J (1981) The dorsal lateral geniculate nucleus of the normal ferret and its postnatal development. J Comp Neurol 203:189–211.

Mesulam M-M (1978) Tetramethyl-benzidine for horseradish peroxidase neurohistochemistry: a non-carcinogenic blue reaction product with superior sensitivity for visualizing neural afferents and efferents. J Histochem Cytochem 26:106–117.

Morgan JE, Henderson Z, Thompson ID (1987) Retinal decussation patterns in pigmented and albino ferrets. Neuroscience 20:519–535.

Payne BR (1990) The representation of the ipsilateral visual field in the transition zone between areas 17 and 18 of the cat's cerebral cortex. Vis Neurosci 4:445–474.

Payne BR, Siwek DF (1991) Visual-field map in the callosal recipient zone at the border between areas 17 and 18 in the cat. Vis Neurosci 7:221–236.

Pettigrew JD, Dreher B (1987) Parallel processing of binocular disparity in the cat's retinogeniculate pathways. Proc R Soc Lond [Biol] 232:297–321.

Pettigrew JD, Ramachandran VS, Bravo H (1984) Some neural connections subserving binocular vision in ungulates. Brain Behav Evol 24:65–93.

Purves D, Lichtman JW (1985) Principles of neural development. Sunderland, MA: Sinauer.

Redies C, Diksic M, Riml H (1990) Functional organization in the ferret visual cortex: a double-label 2-deoxyglucose study. J Neurosci 10:2791–2803.

Rockland KS (1985) Anatomical organization of primary visual cortex (area 17) in the ferret. J Comp Neurol 241:225–236.

Rosa MGP (1997) Visuotopic organization of primate extrastriate cortex. In: Cerebral cortex, Vol 12, Extrastriate cortex in primates (Rockland KS, Kaas JH, Peters A, eds), pp 127–204. New York: Plenum.

Rosenquist AC (1985) Connections of visual cortical areas in the cat. In: Cerebral cortex, Vol 3, Visual cortex (Peters A, Jones EG, eds), pp 81–118. New York: Plenum.

Schall JD, Ault SJ, Vitek DJ, Leventhal AG (1988) Experimental induction of an abnormal ipsilateral visual field representation in the geniculocortical pathway of normally pigmented cats. J Neurosci 8:2039–2048.

Shatz C (1977) A comparison of visual pathways in Boston and midwestern Siamese cats. J Comp Neurol 171:205–228.

Swindale NV (1996) The development of topography in the visual cortex: a review of models. Network Comput Neural Syst 7:161–247.

Thompson ID, Morgan JE (1993) The development of retinal ganglion cell decussation patterns in postnatal pigmented and albino ferrets. Eur J Neurosci 5:341–356.

Thompson ID, Jeffery G, Morgan JE, Baker G (1991) Albino gene dosage and retinal decussation patterns in the pigmented ferret. Vis Neurosci 6:393–398.

Tusa RJ, Rosenquist AC, Palmer LA (1979) Retinotopic organization of areas 18 and 19 in the cat. J Comp Neurol 185:657–678.

Van Essen DC (1979) Visual areas of the mammalian cerebral cortex. Annu Rev Neurosci 2:227–264.

Van Essen DC (1985) Functional organization of primate visual cortex. In: Cerebral cortex, Vol 3, Visual cortex (Peters A, Jones EG, eds), pp 259–329. New York: Plenum.

Vitek DJ, Schall JD, Leventhal AG (1985) Morphology, central projections, and dendritic field orientation of retinal ganglion cells in the ferret. J Comp Neurol 241:1–11.

Volchan E, Bernardes RF, Rocha-Miranda CE, Gleiser L, Gawryszewski LG (1988) The ipsilateral field representation in the striate cortex of the opossum. Exp Brain Res 73:297–304.

White LE, Williams SM, Bosking WH, Richards A, Purves D, Fitzpatrick D (1997) Organization of ocular dominance and orientation preference in areas V1 and V2 of the ferret. Soc Neurosci Abstr 23:1668.

White LE, Bosking WH, Fitzpatrick D (1998) Functional architecture of ferret visual cortex: thalamic inputs to identified ocular dominance territories. Soc Neurosci Abstr 24:1755.

Whitteridge D, Clarke PBH (1982) Ipsilateral visual field represented in the cat's visual cortex. Neuroscience 7:1855–1860.

Wingate RJT, FitzGibbon T, Thompson ID (1992) Lucifer yellow, retrograde tracers, and fractal analysis characterise adult ferret retinal ganglion cells. J Comp Neurol 323:449–474.

Zahs KR, Stryker MP (1985) The projection of the visual field onto the lateral geniculate nucleus of the ferret. J Comp Neurol 241:210–224.